Mechanical Stability of Single DNA Molecules

Hauke Clausen-Schaumann,* Matthias Rief,† Carolin Tolksdorf,* and Hermann E. Gaub*
*LMV–München, Lehrstuhl für Angewandte Physik and Center for Nanoscience, 80799 Munich, Germany, and †Department of Biochemistry B400, Stanford University School of Medicine, Stanford, California 94305-5307 USA

ABSTRACT Using a modified atomic force microscope (AFM), individual double-stranded (ds) DNA molecules attached to an AFM tip and a gold surface were overstretched, and the mechanical stability of the DNA double helix was investigated. In λ-phage DNA the previously reported B-S transition at 65 piconewtons (pN) is followed by a second conformational transition, during which the DNA double helix melts into two single strands. Unlike the B-S transition, the melting transition exhibits a pronounced force-loading-rate dependence and a marked hysteresis, characteristic of a nonequilibrium conformational transition. The kinetics of force-induced melting of the double helix, its reannealing kinetics, as well as the influence of ionic strength, temperature, and DNA sequence on the mechanical stability of the double helix were investigated. As expected, the DNA double helix is considerably destabilized under low salt buffer conditions (≤10 mM NaCl), while high ionic strength buffers (1 M NaCl) stabilize the double-helical conformation. The mechanical energy that can be deposited in the DNA double helix before force induced melting occurs was found to decrease with increasing temperature. This energy correlates with the base-pairing free enthalpy $\Delta G_{bp}(T)$ of DNA. Experiments with pure poly(dG-dC) and poly(dA-dT) DNA sequences again revealed a close correlation between the mechanical energies at which these sequences melt with base pairing free enthalpies ΔG_{bp}(sequence): while the melting transition occurs between 65 and 200 pN in λ-phage DNA, depending on the loading rate, the melting transition is shifted to ~300 pN for poly(dG-dC) DNA, whereas poly(dA-dT) DNA melts at a force of 35 pN.

INTRODUCTION

With the development of new experimental tools allowing piconewton force resolution and Ångstrøm precision positioning of force sensors, mechanical experiments with single molecules have become possible (Binnig et al., 1986; Florin et al., 1994; Kasas et al., 1997; Lee et al., 1994; Merkel et al., 1999; Moy et al., 1994; Radmacher et al., 1994; Rief et al., 1997a; Smith et al., 1992). Such experiments have not only given new insights into intra- and intermolecular forces; they have also shown variations in physical parameters of individual molecules with respect to the mean values derived from ensemble measurements (Perkins et al., 1997; Smith et al., 1992). Furthermore, by investigating single polymers far from their maximum-entropy conformation, these experiments have inspired new concepts in polymer physics, which go far beyond the classical models of this field and incorporate enthalpic deformation and conformational transitions of polymers (Ahsan et al., 1998; Heymann and Grubmüller, 1999; Marko, 1997, 1998; Marszalek et al., 1998; Rief et al., 1997b, 1998).

Early on, the mechanical properties of DNA attracted the interest of both physicists and biologists, because of their importance to numerous biological processes, such as DNA transcription, gene expression and regulation, and DNA replication. Early stretching experiments with single DNA molecules investigated the influence of electrostatic screening on the persistence length (Smith et al., 1992) as well as the hydrodynamic coupling between DNA and the surrounding fluid (Perkins et al., 1995, 1997). As higher forces could be applied to the molecule, a highly cooperative conformational transition was discovered, where the natural B-DNA is converted into a new overstretched conformation called S-DNA (Bensimon et al., 1995; Cluzel et al., 1996; Smith et al., 1996). New theoretical models, as well as molecular dynamics simulations, have shed light on the molecular details of this overstretching transition (Ahsan et al., 1998; Konrad and Bolonick, 1996; Kosikov et al., 1999; Lebrun and Lavery, 1996; MacKerell and Lee, 1999; Marko, 1997, 1998), and the role of twist stored within the double helix has been investigated both experimentally and theoretically (Allemand et al., 1998; Marko, 1997, 1998; Strick et al., 1996, 1998). More recently, unzipping experiments with individual lambda DNA molecules have demonstrated a correlation between the unzipping forces and the average GC and AT content of the unzipped segment of the molecule (Bockelmann et al., 1997; Essevaz-Roulet et al., 1997), and the unzipping of pure CG and AT sequences directly revealed the sequence-specific base pairing forces in DNA (Rief et al., 1999). Finally, DNA transcription by RNA polymerase (Wang et al., 1998; Yin et al., 1995) and binding of RecA to DNA (Hegner et al., 1999; Léger et al., 1998) could be directly investigated under native conditions with single-molecule force experiments.

In this study we investigate the mechanical stability of single DNA molecules as a function of stretching velocity, buffer composition, temperature, and DNA sequence, using AFM-based single molecule force spectroscopy. Furthermore, the kinetics of the force-induced melting of the dou-

Received for publication 7 September 1999 and in final form 18 November 1999.

Address reprint requests to Dr. Hermann E. Gaub, Lehrstuhl für Angewandte Physik, Amalienstrasse 54, 80799 München, Germany. Tel.: +49-89-2180-3172; Fax: +49-89-2180-2050; E-mail: gaub@physik.uni-muenchen.de.

0006-3495/00/04/1997/11 $2.00

ble helix, as well as its reannealing kinetics, are directly investigated.

MATERIALS AND METHODS

λ-BstE II digest DNA (length distribution 117-8454 bp) was purchased from Sigma (Deisenhofen, Germany). Duplex poly(dG-dC) (average length 1257 bp) and poly(dA-dT) (average length 5090 bp) were purchased from Pharmacia (Freiburg, Germany). For the preparation of dsDNA samples, the DNA was used as received and diluted with Tris (Sigma) buffer containing 150 mM NaCl, 10 mM Tris (pH 8), 1 mM EDTA (Sigma) to a final concentration of 100 μg/ml. The DNA was allowed to adsorb to a freshly evaporated gold surface from a 100-μl drop of the 100 μg/ml DNA solution (24-h incubation, ambient temperature), or alternatively, a 100-μl drop of a 100 μg/ml DNA solution was allowed to dry on the gold surface. Prior to the experiments the samples were rinsed with buffer solution containing no DNA, to remove excess DNA from the sample surface. Single-stranded DNA was obtained by dialyzing double-stranded λ-BstE II digest DNA against Millipore water (Millipore Systems, Molsheim, France). The sample was prepared as described for dsDNA, with all preparation steps carried out in Millipore water instead of Tris buffer.

The samples were mounted in a custom-built AFM (Oesterhelt et al., 1999) with a piezo translator with a *z*-range of 6.7 μm. The piezo extension was controlled with a built-in strain gauge. Individual DNA molecules were picked up from the sample with untreated Si_3N_4 AFM tips (Microlevers; Park Scientific Instruments, Sunnyvale, CA) by the application of a contact force of several nanonewtons (nN) for a few seconds, before the piezo was retracted and a DNA molecule was stretched between the gold surface and the AFM tip. The resulting force profile was measured via the deflection of the AFM cantilever spring, using optical lever detection (Amer and Meyer, 1988). Before the first approach of the AFM tip to the surface, the spring constant of each lever was calibrated by measuring the amplitude of its thermal oscillations (Butt and Jaschke, 1995; Florin et al., 1995). The sensitivity of the optical lever detection was then measured by indenting a hard surface with the AFM tip (i.e., by choosing a spot on the substrate where no DNA had been incubated). The spring constants varied between 7 and 15 mN/m, and the resonance frequencies of the cantilevers in buffer varied accordingly between 700 Hz and 1.1 kHz. The sampling rate of the AFM was 60 kHz, and the input signal was filtered at 10 kHz, using an 8-pole low-pass Bessel filter with a cutoff of 48 dB per octave (Frequency Devices, Haverhill, MA). Each force curve consists of 4096 steps. Up to 200 data points were recorded per step, depending on the chosen velocity. For the graphic presentation a box smoothing window (width ≤21 steps) was applied to the data. All experiments were conducted in Tris-EDTA buffer (see above) at 20°C, unless otherwise specified.

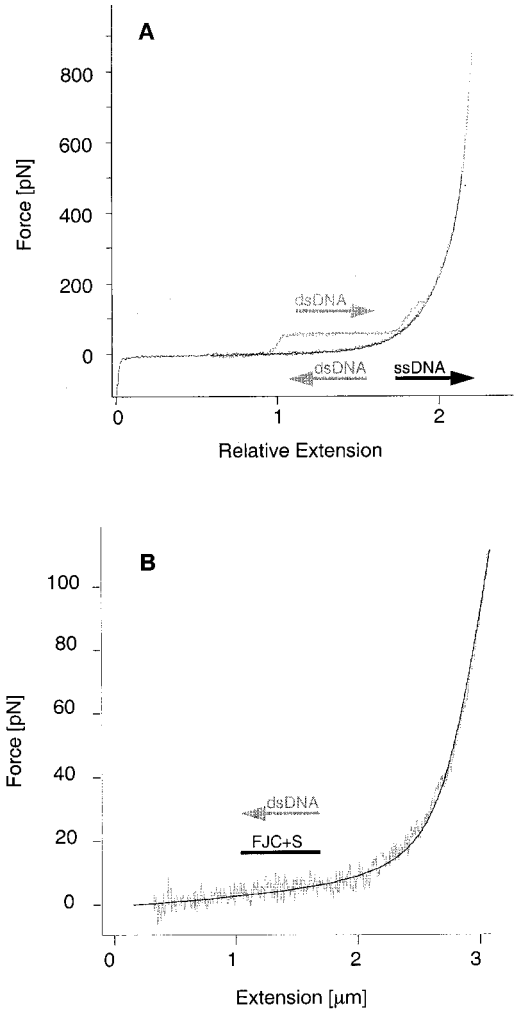

FIGURE 1 (*A*) Stretching and relaxation curve (*gray curves*) of a 1.5-μm-long segment of double-stranded λ-BstE II digest DNA in 150 mM NaCl, 10 mM Tris (pH 8), 1 mM EDTA at an ambient temperature of 20°C. After the highly cooperative B-S transition at 65 pN, a second conformational transition can be observed at around 150 pN, during which the DNA double helix melts and only one of the two strands remains attached between AFM tip and substrate. Superimposed is a force-versus-distance curve of a 300-nm segment of ssDNA (*black curve*) recorded under the same buffer conditions. Because of the different contour lengths of the two molecules, the force curves were scaled to the same relative extension, before superposition. (*B*) Low-force regime of the relaxation curve of the λ digest segment shown in *A* (*gray curve*) and a fit using an extensible FJC model. The fit parameters are the same as those determined for ssDNA, namely a Kuhn length of 15 Å and a stretch modulus of 800 pN (Smith et al., 1996).

RESULTS AND DISCUSSION

When a single λ-digest DNA molecule is stretched beyond the previously described, highly cooperative B-S transition at 65 pN (cf. Fig. 1 *A*, *upper gray curve*), a new conformational transition occurs at ~150 pN (Rief et al., 1999). At the end of this second transition the force increases drastically upon further extension of the molecule. Upon subsequent relaxation of the molecule the force drops continuously, following a smooth curve, exhibiting none of the conformational transitions of the extension curve (Fig. 1 *A*, *lower gray curve*). This marked hysteresis indicates that a massive topological change occurs during this second transition. Moreover, the relaxation curve of the molecule strongly resembles the force versus extension curve of single-stranded DNA (ssDNA), which is free of hysteresis and follows a simple polymer elastic model without conformational transitions (Smith et al., 1996). To illustrate this resemblance to ssDNA, we superimposed a deformation trace of ssDNA (Fig. 1 *A*, *black curve*) on top of the relaxation curve obtained from the double-stranded molecule (*lower gray curve*); the agreement between the two

curves is almost perfect, and they are virtually indistinguishable. This agreement leads us to the interpretation that the high force transition is a force-induced melting transition during which the double helix is split into single strands and only one of the two strands remains attached between the AFM tip and the substrate. In fact, fitting a freely jointed chain (FJC) model with an additional segment elastic modulus (Smith et al., 1992)

$$Ex(F) = L_{ss}\left[\coth\left(\frac{Fb}{k_BT}\right) - \left(\frac{k_BT}{Fb}\right)\right]\left(1 + \frac{F}{S}\right), \qquad (1)$$

to the low-force regime of the relaxation curve obtained from the double-stranded molecule (cf. Fig. 1 *B*) yields a Kuhn length b of 15 Å and a linear segment elasticity S of 800 pN. These parameters are the same as those found by Smith et al. (1996) to model the elastic response of single-stranded DNA. This good agreement with previous studies further corroborates our interpretation that indeed one of the two strands does melt off during the high-force conformational transition. Nevertheless, it is important to note that at forces beyond 100 pN, the linear model used above fails to describe the elastic response of single-stranded DNA. Here nonlinear enthalpic contributions, such as extreme bond angle deformations or bond length variations, seem to become important, and thus quantum chemical and molecular dynamic simulations should be able to provide insight into the molecular details at these forces. Furthermore, it should be noted that the covalent bonds in the backbone of single-stranded DNA sustain forces of at least 0.8 nN, consistent with recent experiments by Grandbois et al. in which the mechanical stability of individual covalent bonds was measured (Grandbois et al., 1999).

More generally, mechanical overstretching and subsequent force-induced melting of the DNA double helix can also lead to different results, depending on the details of the attachment of the molecule to the AFM tip and the gold substrate. If the molecule is attached to the substrate by only one of its two strands and is picked up by the AFM tip at the complementary strand (i.e., the molecule is attached to the substrate and to the AFM tip with both of its 3′ ends or both of its 5′ ends), the connection will be lost upon force-induced melting of the double helix. This can be observed in a number of cases. In other cases, as in the trace shown in Fig. 1 *A*, permanent conversion to single-stranded DNA occurs upon overstretching. Here it is possible that single-strand breaks (nicks) in the DNA strand that melts off, as well as detachment of this strand from the AFM tip and the gold substrate, facilitate complete detachment of the strand and render recombination of the double helix upon relaxation of the molecule impossible. In some cases only a part of the molecule recombines to its double-helical conformation, indicating that only a part of the strand that melts off remains connected to the substrate or to the AFM tip. In most relaxation traces, however, reannealing into a complete double helix can be observed. In such a case (cf. Fig. 2) repeated splitting and reannealing can be performed up to several hundred times with the same molecule. Here the whole strand that melts off must remain attached to one of the two opposing surfaces, or in the presence of a nick it must remain attached to both surfaces. Finally, if the molecule is attached by both strands to both surfaces (tip and substrate) and no single-strand break is present in the molecule, no conversion to ssDNA should be possible, and the hysteresis between extension and relaxation trace should be

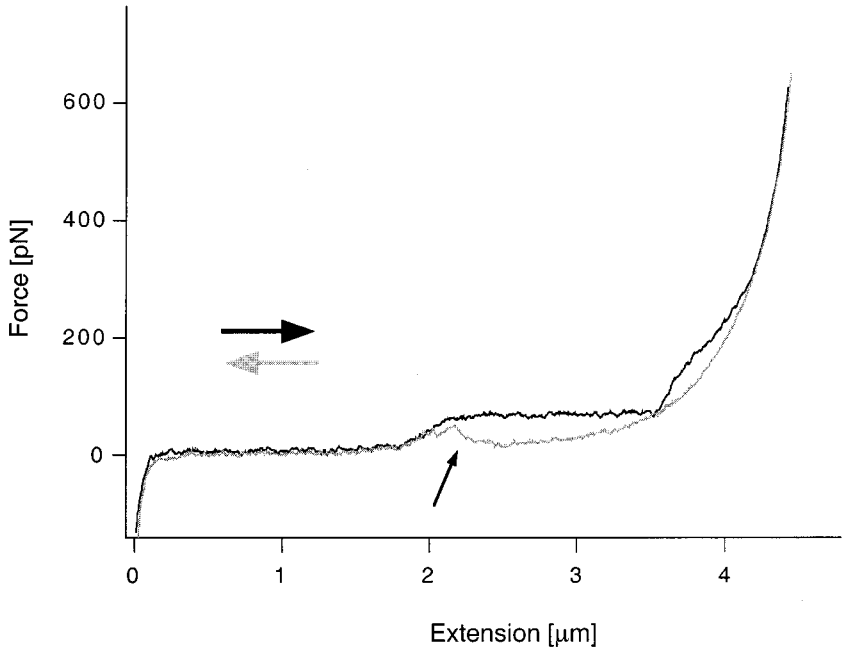

FIGURE 2 Stretching (*black curve*) and relaxation curve (*gray curve*) of a segment of λ-BstE II digest DNA in 150 mM NaCl, 10 mM Tris (pH 8), 1 mM EDTA at an ambient temperature of 20°C. Only after the molecule has been relaxed to ~1.2 times its contour length (see *arrow*) does reannealing into the double-helical conformation occur. Before this overstretching and relaxation cycle, the molecule had been forced trough more than 70 such cycles.

small. Fig. 3 shows an extension-relaxation cycle obtained again on λ-digest DNA, where the first conformational transition is shifted to 105 pN and exhibits significantly less cooperativity than in the trace shown in Fig. 1 *A*: the plateau starts at ~96 pN and ends at 110 pN. At higher forces a second transition can again be observed, but now the molecule shows almost no hysteresis upon relaxation. The changes in the low-force conformational transition of this force curve, when compared to Fig. 1 *A*, are in good agreement with what was predicted by Marko (1998) for a double-stranded DNA molecule with no rotational degree of freedom around the molecule's axis. This has recently been confirmed experimentally by Léger et al. (1999), and experiments with circular closed plasmid DNA in our own laboratory (manuscript in preparation) further corroborate this interpretation of the 105-pN plateau in Fig. 3. Since the rotation of the molecule around its axis is only constrained when the molecule is attached by both strands to both surfaces and when both strands are intact, we conclude that this is indeed the case for force curves, such as the one shown in Fig. 3, with the first conformational transition at ~105 pN. In our experiments, however, we observe such a behavior for less than 5% of all molecules probed, which we attribute to the number of nicks in the DNA samples as well as the attachment of the molecules (see Materials and Methods for details).

An interesting thermodynamic difference between the B-S transition and the melting transition is displayed in Fig. 4, where four extension traces, which were recorded with the same molecule at different pulling velocities, are superimposed on top of each other. Within the experimentally accessible limits, the force of the B-S transition is independent of pulling velocities, whereas the melting transition exhibits a pronounced speed dependence. For a pulling velocity of 3 μm/s the melting transition starts at ~200 pN and ends at ~300 pN, while at pulling velocities of 150 nm/s the molecule seems to transform almost continuously to the single-stranded conformation at the end of the B-S plateau, without the distinct melting transition found in the faster experiments. This shows that the B-S transition is an equilibrium process on the time scale of our experiments, whereas the melting transition occurs in nonequilibrium. In other words, the rearrangement of the helix in the B-S transition occurs much faster than reannealing of the split strands. In view of the complex topology of the molecular rearrangements during the melting transition, this finding is quite intuitive. In contrast to the B-S transition, where only internal rearrangements of the double helix, such as restacking of the bases and a partial unwinding of the helix, are taking place (Kosikov et al., 1999; Lebrun and Lavery, 1996), the two strands have to separate upon melting. The molten strand presumably rotates around the stretched strand and is then likely to assume a random coil conformation with possible intrastrand hairpins (Rief et al., 1999). Upon relaxation this sequence has in one way or another to occur in reverse order. This typically gives rise to a large hysteresis and often even requires nearly complete relaxation of the molecule before reannealing of the double helix is observed (cf. also Fig. 2).

This fact, that at high pulling velocities we observe a melting transition at forces significantly higher than 65 pN, while at slow pulling velocities the melting seems to occur directly at the end of the B-S transition, therefore might imply the existence of an energy barrier for the melting of

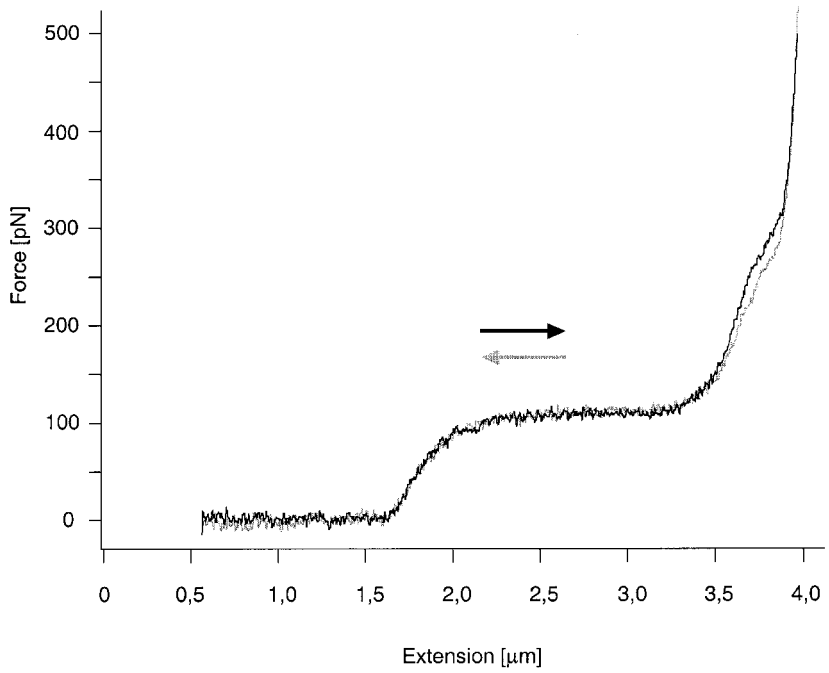

FIGURE 3 Stretching (*black curve*) and relaxation curve (*gray curve*) of a segment of λ-BstE II digest DNA without nicks and with both strands firmly attached to the AFM tip and the substrate surface. Buffer conditions: 150 mM NaCl, 10 mM Tris (pH 8), 1 mM EDTA, 20°C. Here the plateau of the first conformational transition occurs at 105 pN (*middle of the plateau*).

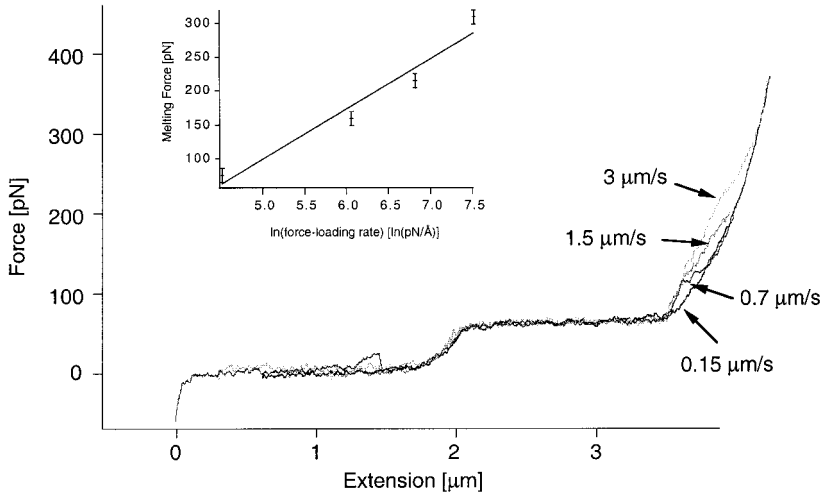

FIGURE 4 Superposition of four extension traces of the same piece of λ-BstE II digest DNA at different pulling velocities: 3, 1.5, 0.7, and 0.15 μm/s. The force at which the melting transition occurs depends on the pulling velocity, ranging from 68 pN at 0.15 μm/s to ~300 pN at 3 μm/s. *Inset*: Melting force versus logarithm of the force loading rate.

the DNA double helix. Two simple explanations for the origin of such an energy barrier are hydrodynamic friction or a static activation barrier to strand separation, as is found for the separation of receptor-ligand pairs (Evans and Ritchie, 1997; Merkel et al., 1999) or short oligonucleotides (Strunz et al., 1999). For a simple kinetic barrier due to hydrodynamic friction one should expect a linear dependence of the melting force on the pulling velocity. However, estimates of the hydrodynamic friction occurring in DNA strand separation (Bockelmann et al., 1997) show that hydrodynamics alone cannot account for forces of 100 pN and more, even at high pulling velocities. This is further corroborated by the fact that even at pulling velocities of 3 μm/s the macroscopic AFM cantilever (a 300-μm-long triangle with 10-μm-wide arms) is deflected only by the equivalent of ~20 pN. For a static activation barrier, on the other hand, a logarithmic dependence of the melting force on the force loading rate might be expected (Evans and Ritchie, 1997; Hänggi et al., 1990; Merkel et al., 1999). However, plotting the melting forces versus the logarithm of the force loading rates (cf. Fig. 4, *inset*) reveals that this again does not explain the data adequately. Apparently, the force-induced melting of the DNA double helix is a more complex process, which cannot be explained by such simplistic models and which may involve multiple steps, such as nucleation, sequential opening of the DNA base pairs, rotation, and random coil formation.

Correlating the velocity dependence of the melting force to the length of the stretched molecule can provide insight into the kinetics of the force-induced melting process of DNA. There is, however, a more direct way to gain information on the kinetics of the melting as well as the reannealing process of the DNA double helix. If the molecule is forced through fast deformation and relaxation cycles, and if different waiting times are introduced at one end of such a cycle, the length of the B-S plateau, which is characteristic for the double-helical conformation of the molecule, should be a measure of how many base pairs were able to melt or reanneal during such a cycle as a function of the waiting time. Fig. 5 *A* shows three extension-relaxation cycles that were obtained for the same dsDNA molecule. In the first cycle the molecule is stretched and relaxed in 112 ms (time for the full cycle) without any waiting time. As can be seen from the lack of hysteresis in the B-S plateau region, during this fast cycle the entire DNA double helix remains intact. If a waiting time of 100 ms is introduced at the fully extended position, because of partial melting of the DNA double helix, the B-S plateau shortens by ~25% in the relaxation curve. Thus, during the 100 ms ~25% of the molecule corresponding to ~2 kb has been able to separate, which corresponds to a force-induced melting rate of ~20 kb/s. In the third cycle the waiting time is increased to 500 ms, and now the entire double helix has been able to melt, resulting in a relaxation trace that exhibits no B-S plateau but follows a curve typical for ssDNA. This corresponds to a melting rate of more than 15 kb/s for the entire DNA segment probed. One should point out that the melting rates vary considerably between experiments conducted on different DNA segments, most likely because of variations in DNA sequence and topology, but also because of slight variations in the experimental conditions. Nevertheless, in these stretching experiments melting rates are consistently larger than 1 kb/s. A similar kind of experiment can be performed to investigate the kinetics of the reannealing process. Here a molecule is stretched through the melting transition and kept at the fully extended position for several seconds to ensure complete melting of the double helix. The molecule is then relaxed and immediately stretched again in a 112-ms cycle (cf. Fig. 5 *B*, *first cycle*). In this case ~35% of the molecule has been able to reanneal to the double-helical conformation. If a waiting time of 100 ms is introduced close to the fully relaxed conformation of the molecule (Fig. 5 *B*, *second cycle*), 60% of the molecule has been able to recombine. Thus, because of the extra 100 ms an

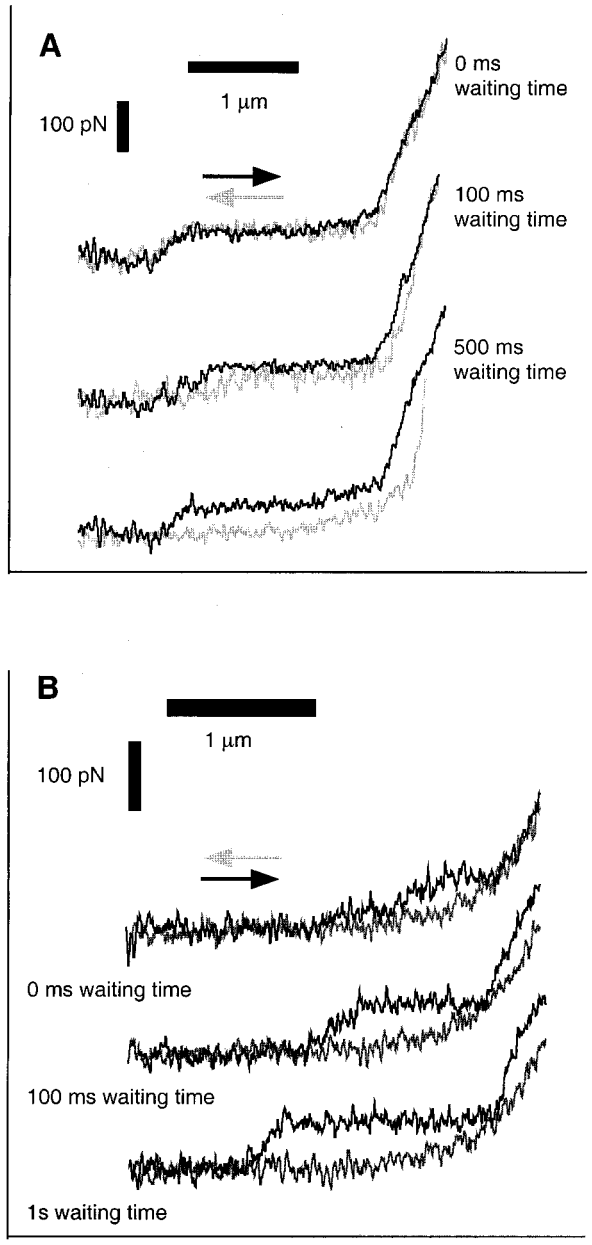

FIGURE 5 (*A*) Three fast stretching and relaxation cycles obtained from the same piece of λ-BstE II digest DNA in 150 mM NaCl, 10 mM Tris (pH 8), 1 mM EDTA at 20°C. In the first cycle the molecule is stretched and immediately relaxed again in a 112-ms cycle. In the second cycle a waiting time of 100 ms is introduced at the fully extended position, and ~25% of the molecules are converted to the single-stranded conformation, as can be seen from the hysteresis in the B-S plateau. If the waiting time at the fully extended position is increased to 500 ms (third cycle), the entire piece of DNA is converted to ssDNA, as can be seen from the lack of a B-S plateau in the relaxation curve. (*B*) Three fast deformation cycles of λ-BstE II digest DNA (same buffer as above). Now the molecule is first stretched to the fully extended position (data not shown), where it is allowed to rest for several seconds to ensure complete melting of the double helix. Then the molecule is relaxed and immediately stretched again in a 112-ms cycle (first cycle). During this fast cycle ~30% of the molecules are able to recombine to the double-helical conformation, as can be seen from the partial appearance of a B-S plateau in the extension curve. If a resting time of 100 ms is introduced in the relaxed position, ~60% are able to recombine, and if the resting time is increased to 1 s, the full B-S plateau reappears, indicating that 100% of the DNA is able to recombine to the double-helical conformation.

additional 25% of the molecule, corresponding to ~1.6 kb, has been able to recombine. This corresponds to a reannealing rate of the DNA double helix of 1.6 kb/s. If the waiting time is increased to 1 s (Fig. 5 *B*, *third cycle*), 100% of the molecule recombines and adopts the double-helical conformation, which leads to a lower estimate of the reannealing rate of 6.5 kb/s (1 s is more time than is needed for reannealing of the entire DNA segment). In our reannealing experiments, the determined rates are again subject to some variation between different experiments and different segments of DNA, but the variation is somewhat smaller, as the reannealing process seems to be less dependent on small variations in the experimental conditions, such as pulling velocities and the exact position of the minimum and maximum extension of the piezo relative to the molecule's conformational transitions. Typical reannealing rates vary between 10 and 20 kb/s. This value for the reannealing rate of the DNA double helix is above the values determined in ensemble measurements, which give a lower limit of 1 kb/s for the DNA hybridization kinetics (James, 1984). Nevertheless, 1 kb/s is considered to be the lower limit for the DNA hybridization kinetics (Blackburn and Gait, 1996), and an important difference between the single-molecule force experiments and ensemble measurements is the fact that in the force experiments the DNA hybridization is clearly a reaction rate-limited process, which allows for direct measurement of the hybridization rate, whereas in 3-D ensemble experiments diffusion may also contribute, and its effect on the measured rates has to be carefully considered.

Another parameter with a strong influence on the mechanical stability of DNA is the ionic strength of the buffer solution. Fig. 6 shows typical force-versus-distance curves of λ-BstE II digest DNA under high and low ionic strength buffer conditions at an ambient temperature of 20°C. In high salt buffer (1 M NaCl, 10 mM Tris (pH 8), 1 mM EDTA) (Fig. 6 *A*) the hysteresis in both B-S and melting transition is significantly less pronounced, and irreversible melting of the double helix can rarely be observed. In low-salt buffers (10 mM NaCl, 10 mM Tris, 1 mM EDTA), on the other hand (Fig. 6 *B*), the hysteresis is very pronounced, and during relaxation the DNA remains in the single-stranded conformation until the molecule is completely relaxed, before the double helix can recombine. Furthermore, under low-salt buffer conditions irreversible conversion to ssDNA is frequently observed. If NaCl is completely removed from the buffer (10 mM Tris, 1 mM EDTA), typically parts or even all of the molecule seems to have denatured even before overstretching of the molecule, and thus only a short overstretching plateau can be ob-

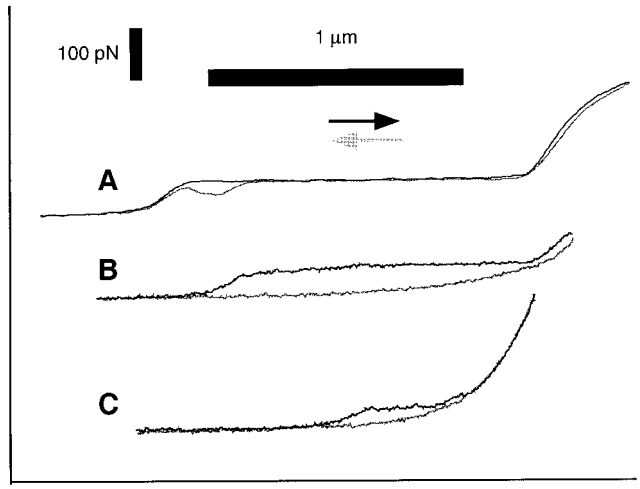

FIGURE 6 Three force versus distance cycles of three pieces of λ-BstE II digest DNA in (*A*) 1 M NaCl, 10 mM Tris (pH 8), 1 mM EDTA; (*B*) 10 mM NaCl, 10 mM Tris (pH 8), 1 mM EDTA; and (*C*) 10 mM Tris (pH 8), 1 mM EDTA. In 1 M NaCl the B-S transition occurs at 65 pN, and the molecule exhibits only a small hysteresis between the extension and relaxation traces. In 10 mM NaCl the B-S plateau starts around 50 pN and rises to 65 pN at the end of the B-S plateau. The molecule exhibits a marked hysteresis, and irreversible conversion to ssDNA is frequently observed. In pure Tris EDTA buffer, without NaCl, usually large parts of the molecules denature as soon as they are stretched, and very short or no B-S plateaus can be observed.

served, corresponding to small and presumably GC-rich parts of the molecule that are still in a double-helical conformation (cf. Fig. 6 *C*). This result is consistent with the fact that the electrostatic repulsion between the negatively charged phosphate groups along the backbone of each of the two strands is effectively screened at a salt concentration of 1 M, where the Debye screening length is smaller than the B-DNA diameter of 2 nm (Israelachvili, 1992; Voet and Voet, 1995). Another interesting difference between the force-distance curves obtained in low- and in high-salt buffers is the fact that in 1 M NaCl the B-S plateau is highly cooperative and occurs at 65 pN, just as in 150 mM NaCl, while in 10 mM NaCl the B-S plateau typically starts at ~50 pN and rises to 65 pN at the end of the B-S transition. For the 10 mM Tris buffer without NaCl, the B-S plateau starts at 40 pN and quickly rises to ~65 pN. This low onset of the B-S plateau under low-salt conditions agrees well with data by Baumann et al., who investigated the first 30% of the B-S plateau in λ-DNA as a function of NaCl concentration (Baumann et al., 1997). Furthermore, in our data, the melting transition is somewhat less pronounced in 10 mM NaCl, when compared to data obtained in 1 M NaCl buffer. This seems to suggest that in 10 mM NaCl buffer, the melting of AT-rich regions of DNA occurs already at forces below 65 pN, while the GC-rich regions still contribute to the distinct force-induced melting transition at higher forces. In the NaCl-free buffer no distinct melting transition can be observed (cf. Fig. 6 *C*).

As already pointed out above, if the pulling velocity is slow enough to allow all necessary conformational rearrangements to take place in a quasistatic manner as the molecule is extended, the DNA double helix seems to melt immediately after the B-S transition. If one compares the mechanical energy deposited in a dsDNA molecule at the end of the B-S plateau with thermodynamic data (Breslauer et al., 1986; Duguid et al., 1996), the surprising result is that at a relative extension of 1.7 (at the end of the B-S plateau), the mechanical energy deposited in the dsDNA molecule already exceeds the base-paring free enthalpy $\Delta G_{bp}(20°C)$ of DNA. Even if the mechanical energy stored in the single strand that remains attached between the AFM tip and the substrate is subtracted from the mechanical energy deposited in the double-stranded molecule, the excess mechanical energy deposited in the double-helical molecule is still comparable to the base-pairing free enthalpy $\Delta G_{bp}(20°C)$ of DNA. This is illustrated in Fig. 7, where a DNA stretching curve ($f_{ds}(z)$) and the relaxation curve ($f_{ss}(z)$) of the remaining single strand (*gray curves*; force axis on the *right side*) of a 2.3-μm piece of dsDNA are shown and the integral $\int(f_{ds}(z) - f_{ss}(z))\cdot dz$ (*black curve*; energy axis on the *left side*) that corresponds to the area between the two curves is compared directly to the thermodynamic data: The dashed line in Fig. 7 represents the base-pairing free enthalpy $\Delta G_{bp}(20°C)$ of a 2.3-μm random DNA segment according to Breslauer et al. (1986). Here the average value of all 10 possible base-pairing enthalpies and entropies given by Breslauer et al. was used to calculate $\Delta G_{bp}(20°C)$ of a random DNA sequence, making use of the equation

$$\Delta G(T) = \Delta H - T \cdot \Delta S. \tag{2}$$

The dotted line in Fig. 7 represents the base-pairing free enthalpy $\Delta G_{bp}(20°C)$ of the same 2.3-μm DNA segment according to Duguid et al. (1996). Unlike Breslauer et al., who determined ΔH_{bp} and ΔS_{bp} of all 10 possible Watson-Crick base pairs, using short synthetic oligonucleotides, Duguid et al. used 160-bp fragments of calf thymus DNA to determine ΔH_{bp} and ΔS_{bp} of a random DNA sequence. To compare the thermodynamic data to the force experiment, the calorimetry data were extrapolated to the salt concentration used in the force experiment (100 mM NaCl), using the equation

$$T_m(C) = T_m(1\ M) + 16.6 \cdot \log C, \tag{3}$$

where T_m is the melting temperature and C is the NaCl concentration (Schildkraut and Lifson, 1965).

It is well known that the stability of DNA decreases with increasing temperature, and that most natural DNA sequences are completely denatured at temperatures around 90°C, in physiological buffer conditions. If the temperature is raised to 40°C and more in a force experiment, typically a distinct melting transition can no longer be observed, even for comparably fast stretching velocities, and the force of

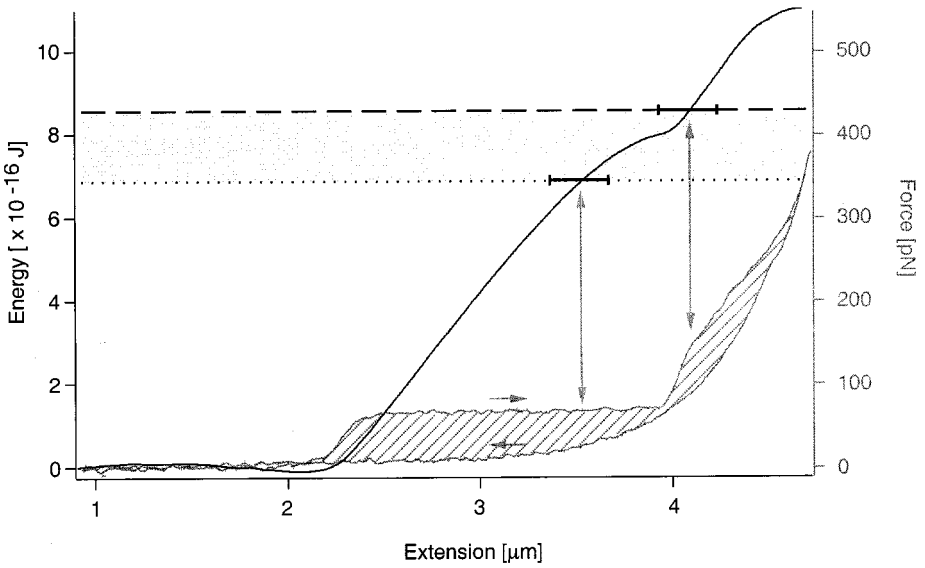

FIGURE 7 Force versus extension cycle (*gray curves*; *force axis on the right*) of a segment of λ-DNA in 100 mM NaCl, 10 mM Tris (pH 8), 1 mM EDTA at 20°C, and the integral $\int(f_{ds}(z) - f_{ss}(z))\cdot dz$ (*continuous black curve, energy axis on the left*) and base-pairing free enthalpies $\Delta G_{bp}(20°C)$ of the 2.3-μm-long DNA segment, according to Breslauer et al. (1986) (– – –) and Duguid et al. (1996) (·····).

the B-S transition is reduced to values below 65 pN (cf. Fig. 8 *A*). If one compares the force values obtained for the B-S plateau as a function of temperature with the thermodynamic data (Breslauer et al., 1986), using Eq. 2, the mechanical energy deposited in the double helix at the end of the B-S plateau is in accordance with the base-pairing free enthalpy $\Delta G_{bp}(T)$. Fig. 8 *B* shows the experimental values of the B-S plateau force as a function of temperature and a linear fit to the data points (*markers* and *black line* in Fig. 8 *B*), compared to the base-pairing free enthalpy $\Delta G_{bp}(T)$. In this graph, all energies are divided by 2.38 Å, which is the length gained per base pair of dsDNA during the B-S transition. This allows direct comparison of the measured plateau height to the base-pairing free enthalpy of DNA. The dashed line in Fig. 8 *B* represents $\Delta G_{bp}(T)$ according to Breslauer et al. (1986). (The thermodynamic data have again been extrapolated to the salt concentration used in the force experiments (150 mM NaCl), using Eq. 3.) Comparing mechanical energies to the base-pairing free enthalpies derived from thermal denaturation experiments, one has to bear in mind that in a typical force experiment one strand of ssDNA remains attached between the AFM tip and the substrate surface. If the mechanical energy stored in ssDNA at an extension of 5.78 Å/bp (this corresponds to the end of the B-S plateau in dsDNA) is subtracted from the B-S plateau forces, the result (*gray line* in Fig. 8 *B*) agrees well with the thermodynamic data: the mechanical energy at the end of the B-S plateau is only slightly less than the base-pairing free enthalpy $\Delta G_{bp}(T)$, and the deviation is still within the experimental errors of the force experiments. If we use the force experiments to determine the thermodynamic parameters of DNA, and making again use of $\Delta G(T) = \Delta H - T\cdot\Delta S$, the ordinate and slope of the black line in Fig. 8 *B* yield a ΔH_{bp} of 10.27 kcal/(mol·bp) and a ΔS_{bp} of 27.04 cal/(mol·bp). The gray line, which also accounts for the remaining single strand, corresponds to a ΔH_{bp} of 10.26 kcal/(mol·bp) and a ΔS_{bp} of 28.70 cal/(mol·bp). These values for ΔH_{bp} are only slightly above the values determined for random DNA sequences in calorimetry experiments (Breslauer et al., 1986; Duguid et al., 1996), and they agree rather well with the values for GC base pairs (Breslauer et al., 1986). On the other hand, the force experiments seem to overestimate the base pairing entropy, because the values for ΔS_{bp} are even larger than the ones determined for GC base pairs by Breslauer et al.

Together with the good agreement between thermodynamic data and the B-S plateau height, the fact that we do not observe a distinct melting transition at high temperatures suggests that at high temperatures a force-induced melting of the DNA double helix already occurs in the B-S transition, whereas at room temperature the DNA starts to melt after the B-S transition: The high cooperativity of the B-S transition has been explained as an all-or-none process, where domains of fully overstretched S-DNA grow with further extension of the molecule, rather than a process where all base pairs in the molecule gradually change their extension until they are fully overstretched to 5.78 Å/bp (Ahsan et al., 1998; Smith et al., 1996). Consequently, if the double-helical conformation is significantly destabilized by an increased temperature, the double helix has to melt in these fully overstretched domains as soon as the molecule is extended into the B-S transition, even if the entire molecule is still in a state of relatively small overstretching. With increasing extension more DNA will then gradually be converted to the single-stranded conformation, while at room temperature the melting process starts at the very end of the B-S plateau, except for AT-rich DNA segments (cf. next paragraph).

As has been pointed out in the last paragraph, not only kinetics, salt concentration and temperature, but also the

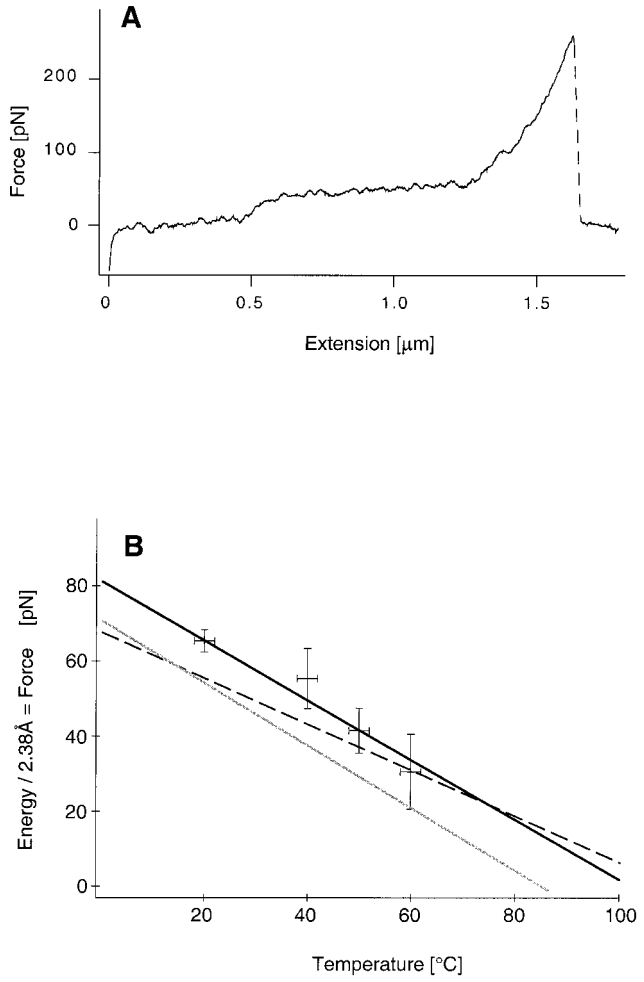

FIGURE 8 (*A*) Force versus extension trace of ds λ-BstE II digest DNA in 150 mM NaCl, 10 mM Tris (pH 8), 1 mM EDTA at 50°C. The B-S plateau occurs at 41 pN, and a distinct melting transition at higher forces cannot be observed. (*B*) B-S-plateau forces (*markers*) versus temperature and a linear fit to the data (*black line*). The gray line represents the fit to the B-S plateau forces minus the mechanical energy deposited in one base of ssDNA at an extension of 5.78 Å, which corresponds to the extension per base pair of dsDNA at the end of the B-S plateau. The dashed line represents the base pairing free enthalpy $\Delta G_{bp}(T)$ per base pair of a random DNA sequence according to Breslauer et al. (1986). All energies are divided by 2.38 Å to compare them directly to the B-S plateau forces, because dsDNA elongates by ~2.38 Å/bp during the B-S transition.

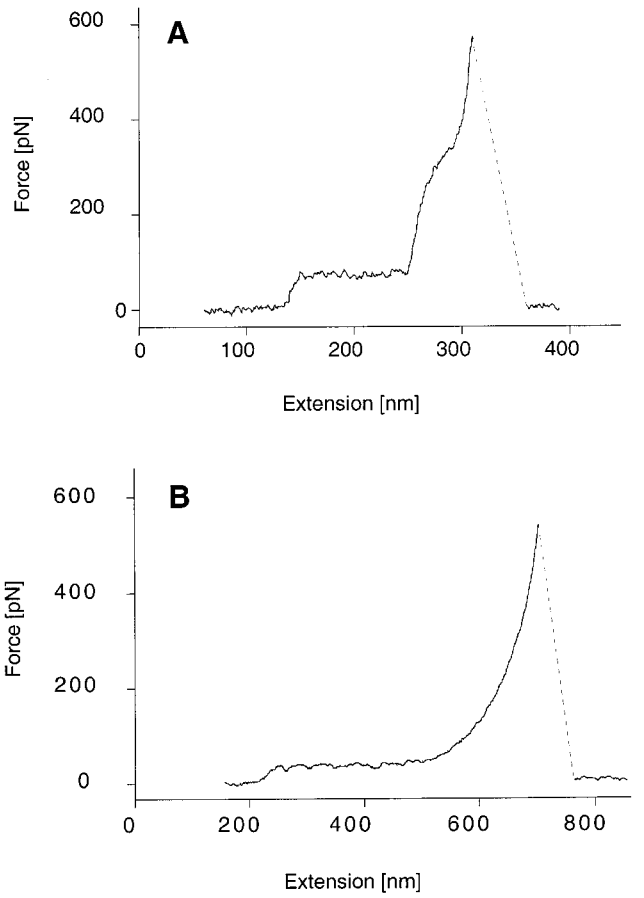

FIGURE 9 Force versus extension traces of poly(dG-dC)·poly(dG-dC) (*A*) and poly(dA-dT)·poly(dA-dT) DNA (*B*) in 150 mM NaCl, 10 mM Tris (pH 8), 1 mM EDTA at 20°C. For the poly(dG-dC) double helix the B-S transition occurs again at 65 pN, while the melting transition is shifted to forces around 300 pN. For poly(dA-dT) DNA the B-S plateau occurs at 35 pN, and no distinct melting transition can be observed.

specific sequence of the stretched DNA molecule should influence its mechanical properties and, in particular, its mechanical stability. To investigate the sequence dependence of the mechanical properties and of the mechanical stability of DNA, we stretched synthetic constructs of double-stranded poly(dG-dC) as well as poly(dA-dT). Fig. 9 shows extension traces during which the molecules were stretched to the maximum attachment force, where the AFM cantilever snaps back to its resting position at zero force. The different sequences exhibit pronounced differences in their conformational transitions. For double-stranded poly(dG-dC) (Fig. 9 *A*) the B-S transition occurs again at 65 pN, just as in λ-DNA, while the melting transition is shifted toward higher forces, starting at ~250 pN and leading into the single-stranded conformation at 350 pN. For poly(dA-dT) DNA (Fig. 9 *B*), however, the force of the first conformational transition is reduced to 35 pN, and, much as at high temperatures, the double helix seems to melt already during this transition, so that an additional melting transition can no longer be observed. This result can again be understood, taking into account that the mechanical energy deposited in the double helix during the 35-pN conformational transition is comparable to the base-pairing free enthalpy of poly(dA-dT)·poly(dA-dT) DNA (Breslauer et al., 1986). This interpretation is further corroborated by the finding that hairpins are formed in the self-complementary poly(dA-dT) sequence already after a molecule has been extended only partially into the B-S transition (Rief et al., 1999). On the other hand, the fact that for the more stable poly(dG-dC)·poly(dG-dC) molecules the B-S transition re-

mains unchanged and only the melting transition is shifted to higher forces is an indication that the value of 65 pN corresponds indeed to the force where the B-S transition occurs naturally. Thus, only if the base pairing free energy $\Delta G_{bp}(T, \text{sequence})$ of a molecule is already exceeded in the B-S transition, melting of the molecule occurs at a force below 65 pN.

CONCLUSION

We have shown that if individual DNA double strands are mechanically overstretched, the double helix melts into single strands that, depending on the attachment of the two strands to the mechanical actuators and on the number of single-strand breaks in the molecule, may recombine to the double-helical conformation upon relaxation of the molecule. The force at which this melting of the double helix occurs depends on the pulling velocity, the ionic strength, and the temperature, as well as on the DNA sequence. The kinetics of this force-induced melting and the reannealing process have been investigated, and it has been shown that on our experimental time scale the covalently closed backbone of a single DNA strand withstands forces of at least 0.8 nN. Furthermore, by varying the temperature as well as the DNA sequence, good agreement was found between the mechanical energies that can be deposited in the DNA molecule before force-induced melting of the double helix occurs and base pairing-free enthalpies ΔG_{bp}, determined in thermal DNA denaturation experiments. Together with the work from other research groups, these results may open the door to new approaches in the investigation of the interaction of DNA with proteins or chemical agents that stabilize or destabilize the double-helical conformation of DNA. Experiments investigating DNA protein interaction as well as the interaction of cytostatics with DNA are currently being conducted in our laboratory.

The authors thank K. Stierstadt, E. Evans, V. Croquette, and D. Chatenay for stimulating discussions.

This work was supported by the Deutsche Forschungsgemeinschaft.

REFERENCES

Ahsan, A., J. Rudnick, and R. Bruinsma. 1998. Elasticity theory of the B-DNA to S-DNA Transition. *Biophys. J.* 74:132–137.

Allemand, J. F., D. Bensimon, R. Lavery, and V. Croquette. 1998. Stretched and overwound DNA forms a Pauling-like structure with exposed bases. *Proc. Natl. Acad. Sci. USA.* 95:14152–14157.

Amer, N. M., and G. Meyer. 1988. A simple method for a remote sensing of stylus deflection in AFM. *Bull. Am. Phys. Soc.* 33:319.

Baumann, C. G., S. B. Smith, V. A. Bloomfield, and C. Bustamante. 1997. Ionic effects on the elasticity of single DNA molecules. *Proc. Natl. Acad. Sci. USA.* 94:6185–6190.

Bensimon, D., A. J. Simon, V. Croquette, and A. Bensimon. 1995. Stretching DNA with a receding meniscus: experiments and models. *Phys. Rev. Lett.* 74:4754–4757.

Binnig, G., C. F. Quate, and C. Gerber. 1986. Atomic force microscope. *Phys. Rev. Lett.* 56:930.

Blackburn, G. M., and M. J. Gait. 1996. Nucleic Acids in Chemistry and Biology. Oxford University Press, Oxford.

Bockelmann, U., B. Essevaz-Roulet, and F. Heslot. 1997. Molecular stick-slip motion revealed by opening DNA with piconewton forces. *Phys. Rev. Lett.* 79:4489–4492.

Breslauer, K. J., R. Frank, H. Blöcker, and L. A. Marky. 1986. Predicting DNA duplex stability from the base sequence. *Proc. Natl. Acad. Sci. USA.* 83:3746–3750.

Butt, H. J., and M. Jaschke. 1995. Thermal noise in atomic force microscopy. *Nanotechnology.* 6:1–7.

Cluzel, P., A. Lebrun, C. Heller, R. Lavery, J.-L. Viovy, D. Chatenay, and F. Caron. 1996. DNA: an extensible molecule. *Science.* 271:792–794.

Duguid, J. G., V. A. Bloomfield, J. M. Benevides, and G. J. Thomas, Jr. 1996. DNA melting investigated by differential scanning calorimetry and Raman spectroscopy. *Biophys. J.* 71:3350–3360.

Essevaz-Roulet, B., U. Bockelmann, and F. Heslot. 1997. Mechanical separation of the complementary strands of DNA. *Proc. Natl. Acad. Sci. USA.* 94:11935–11940.

Evans, E., and K. Ritchie. 1997. Dynamic strength of molecular adhesion bonds. *Biophys. J.* 72:1541–1555.

Florin, E.-L., V. T. Moy, and H. E. Gaub. 1994. Adhesive forces between individual ligand-receptor pairs. *Science.* 264:415–417.

Florin, E. L., M. Rief, H. Lehmann, M. Ludwig, C. Dornmair, V. T. Moy, and H. E. Gaub. 1995. Sensing specific molecular interactions with the atomic force microscope. *Biosens. Bioelectron.* 10:895–901.

Grandbois, M., M. Beyer, M. Rief, H. Clausen-Schaumann, and H. E. Gaub. 1999. How strong is a covalent bond? *Science.* 283:1727–1730.

Hänggi, P., P. Talkner, and M. Borkovec. 1990. Reaction-rate theory: fifty years after Kramers. *Rev. Mod. Phys.* 62:251–341.

Hegner, M., S. B. Smith, and C. Bustamante. 1999. Polymerization and mechanical properties of single RecA-DNA filaments. *Proc. Natl. Acad. Sci. USA.* (in press).

Heymann, B., and H. Grubmüller. 1999. "Chair-boat" transitions and side groups affect the stiffness of polysaccharides. *Chem. Phys. Lett.* 305: 202–208.

Israelachvili, J. N. 1992. Intermolecular and Surface Forces. Academic Press, New York.

James, T. L. 1984. *In* Phosphorus-31 NMR. J. Gorenstein, editor. Academic Press, San Diego. 349–400.

Kasas, S., N. H. Thomson, B. L. Smith, H. G. Hansma, X. Zhu, M. Guthold, C. Bustamante, E. T. Kool, M. Kashlev, and P. K. Hansma. 1997. *Escherichia coli* RNA polymerase activity observed using atomic force microscopy. *Biochemistry.* 36:461–468.

Konrad, M. W., and J. I. Bolonick. 1996. Molecular dynamics simulation of DNA stretching consistent with the tension observed for extension and strand separation and predicts a novel ladder structure. *J. Am. Chem. Soc.* 118:10989–10994.

Kosikov, K. M., A. A. Gorin, V. B. Zhurkin, and W. K. Olson. 1999. DNA stretching and compression: large-scale simulations of double helical structures. *J. Mol. Biol.* 289:1301–1326.

Lebrun, A., and R. Lavery. 1996. Modelling extreme stretching of DNA. *Nucleic Acids Res.* 24:2260–2267.

Lee, G. U., L. A. Chris, and R. J. Colton. 1994. Direct measurement of the forces between complementary strands of DNA. *Science.* 266:771–773.

Léger, J. F., J. Robert, L. Bourdieu, D. Chatenay, and J. F. Marko. 1998. RecA binding to a single double-stranded DNA molecule: a possible role of DNA conformational fluctuations. *Proc. Natl. Acad. Sci. USA.* 95: 12295–12299.

Léger, J. F., G. Romano, A. Sarkar, J. Robert, L. Bourdieu, D. Chatenay, and J. F. Marko. 1999. Structural transitions of a twisted and stretched DNA molecule. *Phys. Rev. Lett.* 83:1066–1069.

MacKerell, A. D., Jr., and G. U. Lee. 1999. Structure, force and energy of a double-stranded DNA oligonucleotide under tensile loads. *Eur. Biophys. J.* 28:415–426.

Marko, J. F. 1997. Stretching must twist DNA. *Europhys. Lett.* 38: 183–188.

Marko, J. F. 1998. DNA under high tension: overstretching, undertwisting and relaxation dynamics. *Phys. Rev. E.* 57:2134–2149.

Marszalek, P. E., A. F. Oberhauser, Y. P. Pang, and J. M. Fernandez. 1998. Polysaccharide elasticity governed by chair-boat transitions of the glucopyranose ring. *Nature.* 396:661–664.

Merkel, R., P. Nassoy, A. Leung, K. Ritchie, and E. Evans. 1999. Energy landscapes of receptor-ligand bonds explored with dynamic force spectroscopy. *Nature.* 397:50–53.

Moy, V. T., E. L. Florin, and H. G. Gaub. 1994. Intermolecular forces and energies between ligands and receptors. *Science.* 266:257–259.

Oesterhelt, F., M. Rief, and H. E. Gaub. 1999. Single molecule force spectroscopy by AFM indicates helical structure of poly(ethyleneglycol) in water. *New J. Phys.* 1:6.1–6.11.

Perkins, T., D. Smith, and S. Chu. 1997. Single polymer dynamics in an elongational flow. *Science.* 276:2016–2021.

Perkins, T. T., D. E. Smith, R. G. Larson, and S. Chu. 1995. Stretching of a single tethered polymer in a uniform flow. *Science.* 268:83–87.

Radmacher, M., M. Fritz, H. G. Hansma, and P. K. Hansma. 1994. Direct observation of enzyme activity with the atomic force microscope. *Science.* 265:1577–1579.

Rief, M., H. Clausen-Schaumann, and H. E. Gaub. 1999. Sequence dependent mechanics of single DNA molecules. *Nature Struct. Biol.* 6:346–349.

Rief, M., J. M. Fernandez, and H. E. Gaub. 1998. Elastically coupled two-level systems as a model for biopolymer extensibility. *Phys. Rev. Lett.* 81:4764–4767.

Rief, M., M. Gautel, F. Oesterhelt, J. M. Fernandez, and H. E. Gaub. 1997a. Reversible unfolding of individual titin Ig-domains by AFM. *Science.* 276:1109–1112.

Rief, M., F. Oesterhelt, B. Heymann, and H. E. Gaub. 1997b. Single molecule force spectroscopy on polysaccharides by AFM. *Science.* 275:1295–1298.

Schildkraut, C., and S. Lifson. 1965. Dependence of the melting temperature of DNA on the salt concentration. *Biopolymers.* 3:195–208.

Smith, S. B., Y. Cui, and C. Bustamante. 1996. Overstretching B-DNA: the elastic response of individual double-stranded and single-stranded DNA molecules. *Science.* 271:795–798.

Smith, S. B., L. Finzi, and C. Bustamante. 1992. Direct mechanical measurements of the elasticity of single DNA molecules by using magnetic beads. *Science.* 258:1122–1126.

Strick, T. R., J. F. Allemand, D. Bensimon, A. Bensimon, and V. Croquette. 1996. The elasticity of a single supercoiled DNA molecule. *Science.* 271:1835–1837.

Strick, T. R., J.-F. Allemand, D. Bensimon, and V. Croquette. 1998. Behavior of supercoiled DNA. *Biophys. J.* 74:2016–2028.

Strunz, T., K. Oroszlan, R. Schäfer, and H.-J. Güntherodt. 1999. Dynamic force spectroscopy of single DNA molecules. *Proc. Natl. Acad. Sci. USA.* 96:11277–11282.

Voet, D., and J. Voet. 1995. Biochemistry. Wiley, New York.

Wang, M. D., M. J. Schnitzer, H. Yin, R. Landick, J. Gelles, and S. M. Block. 1998. Force and velocity measured for single molecules of RNA polymerase. *Science.* 282:902–907.

Yin, H., M. D. Wang, K. Svoboda, R. Landick, S. M. Block, and J. Gelles. 1995. Transcription against an applied force. *Science.* 270:1653–1657.